Stober et al. *Swiss Journal of Geosciences* (2022) 115:3
https://doi.org/10.1186/s00015-021-00403-8

SGG SGS sc | nat
Swiss Journal of Geosciences

ORIGINAL PAPER Open Access

# The deep Basel-1 geothermal well: an attempt assessing the predrilling hydraulic and hydrochemical conditions in the basement of the Upper Rhine Graben

Ingrid Stober[1*], Florentin Ladner[2], Moritz Hofer[1] and Kurt Bucher[1]

**Abstract**

Hydrogeological properties of fluid reservoirs in the brittle continental crust at 5 km have been deduced from hydraulic and chemical data provided by the Deep Heat Mining well Basel-1 in the south of the Upper Rhine rift valley (central Europe, Switzerland). The investigation was challenging because no direct temperature logs or fluid samples from the undisturbed reservoir exist. However, the properties of the undisturbed reservoir have been reliably reconstructed from short time hydraulic tests and the evolution of outflow water composition. The rock of the open hole sections (4629–5000 m) is predominantly coarse-grained undeformed poorly fractured quartz-monzodiorite. The permeability $k = 5.8 \times 10^{-18}$ m$^2$ is characteristic for plutonic basement at 5 km depth. Fluid flow is restricted to few steeply dipping fracture zones in this section. Outflow water triggered by massive injection of river water contains predominantly NaCl. The total of dissolved solids (TDS) in the pristine reservoir at depth is about 45 g kg$^{-1}$. The origin of the high salinity is probably fossil seawater. The water has been modified in the reservoir by desiccation reactions related to the partial and local hydration of the igneous reservoir rock. The estimated reservoir temperature of 185 °C using three different calibrations of standard fluid geothermometers is in excellent agreement with measured and extrapolated temperatures in the borehole. The consistent application of different fluid geothermometers confirms the rock control of the fluid composition.

**Keywords:** Brittle basement, Deep well, Hydrochemistry, Hydraulics, Geothermometer, Permeability

## 1 Introduction

Fractures, faults, joints, and veins, i.e. features of brittle deformation, are the principal water-conducting structures in basement rocks and provide the dominant conduits for fluid flow in the brittle upper continental crust. The fracture pore space of rocks normally forms an interconnected network of open permeable space filled with an aqueous fluid. Deep geothermal energy development extracts this hot fluid via some km deep wells and removes the thermal energy. Pumping tests in the boreholes provide hydraulic information and data including permeability of the reservoir formation. The tests also supply samples of the pumped water for chemical analysis. There is a wealth of well test data from the crystalline basement to 1000 m depth (e.g. Achtziger-Zupancic et al., 2017; Clauser, 1992; Manning & Ingebritsen, 1999; Stober, 1986; Zeitlhöfler et al., 2015). The data show that the hydraulic conductivity of the basement is related to the interconnected open fractures. At greater depth, however, the hydraulic properties of the formation and composition of the fluid are poorly known. Only a few tested wells reaching depths of 4–5 km exist on a worldwide

Editorial handling: Paola Manzotti.

*Correspondence: ingrid.stober@minpet.uni-freiburg.de
[1] Institute of Earth and Environmental Sciences, University of Freiburg, Albertstr. 23b, D-79104 Freiburg, Germany
Full list of author information is available at the end of the article

basis (e.g.; Holl, 2015; Pine & Ledingham, 1983; Pauwels et al., 1993; Stober & Bucher, 2005, 2014; Sanjuan et al., 2016; Solberg et al., 1980; Stober, 2011; Tischner et al., 2006; Vidal & Genter, 2018).

Measured permeability of the upper continental crust varies over a very large range (nine log-units) from $10^{-14}$ to $10^{-4}$ m $s^{-1}$ (Stober & Bucher, 2006), depending on the predominant rock type at the studied site and the geological history of the drilled crystalline basement. This large variance and the permeability itself decrease with depth (e.g. Ingebritsen & Manning, 1999; Stober & Bucher, 2006). The composition of the aqueous fluid, also known as groundwater, residing in the porespace of the basement varies considerably from site to site with regard to the cation and anion distribution and the total dissolved solids (TDS) (e.g. Bucher & Stober, 2010). Generally, TDS increases with depth and groundwater at some depth tends to evolve to Na-(Ca)-Cl brines. Highly saline brines have been described from several km depth in the continental basement worldwide (e.g. Banks et al., 1996; Edmunds & Savage, 1991; Emmermann et al., 1995; Frape & Fritz, 1987; Frape et al., 2004; Pauwels et al., 1993; Stober & Bucher, 1999a; Bucher & Stober, 2010; Sanjuan et al., 2016).

The crystalline basement of the continents consists predominantly of granite and gneiss. Thus, deep water is mostly in contact with K-feldspar, Na-rich plagioclase, quartz, biotite, and various accessory minerals. The interaction of the hot fluid with these minerals contributes to the composition of the deep water (Grimaud et al., 1990; Aquilina et al., Aquilina, Pauwels, et al., 1997, b).

However, the deep water may acquire its solutes by a large variety of different processes including the above mentioned fluid-rock interaction (WRI), the import of fluids from other crustal units, contributions by the cover, and temperature (depth) variations. The origin and composition of recharge can have an effect on the evolution of deep waters. It is difficult to separate the many different contributions to the composition of basement water.

Detailed information on the hydrogeological properties of the deeper parts of the upper continental crust is scarce. Although research drillholes to 9 and 12 km depth exist, natural permeability and uncontaminated water composition from the basement are not known for depths greater than about 5 km (Emmermann et al., 1995; Kozlovsky, 1987).

The deep boreholes at Soultz-sous-Forêts near Strasbourg (Alsace, France) accessed the crystalline basement rocks of the URG. The cores and hydraulic tests in the wells provided detailed knowledge of the hydraulic and hydrochemical properties of the crystalline basement at 200 °C and 5 km depth (e.g. Vidal & Genter, 2018).

The 5 km deep Basel-1 borehole was drilled in the northern part of Basel/Switzerland in the URG in 2006 to create an enhanced geothermal system (EGS) exclusively in crystalline basement rocks. Massive hydraulic stimulation with surface water was carried out in the open hole sections (4629–5000 m depth) to enhance the in-situ permeability. However, high rates of microseismic activity built up during the first days of freshwater injection, followed by two high event magnitudes (max. $M_L = 3.4$), and resulted in abandoning the project (Häring, Ladner, et al., 2008).

Generally, massive hydraulic injection of surface water immediately after the drilling operation in research and deep geothermal wells is typically carried out to enhance the productivity, i.e. to improve the natural permeability. Thus, undisturbed hydraulic and hydrochemical conditions at the site remain unknown.

The general scarcity of data from the deep undisturbed basement and its hydrogeological properties motivated us to analyze the available hydraulic and hydrochemical data of Basel-1. The purpose of the study is the reconstruction of the predrilling conditions at the once planned geothermal reservoir. The paper presents evaluated hydraulic pre-tests assessing the natural permeability of the basement. It also presents rock composition data from cored samples from the open hole section. We collected outflow water samples from the borehole (after the massive hydraulic injection with surface water) for deriving the undisturbed composition of the reservoir fluid. Additionally, leaching experiments with basement rocks provided fluid composition data and kinetic information on fluid rock interaction. The predrilling reservoir temperature has been obtained from the restored original water composition.

The method chapter is presented in the Online Appendix (Additional file 1).

## 2 Geology and temperature of the deep Basel-1 borehole

The Basel-1 borehole in the city of Basel in northern Switzerland near the river Rhine (Fig. 1) is sited close to the SE margin of the Upper Rhine Graben of the European Cenozoic rift system (Dèzes et al., 2004; Laubscher, 2001). Numerous high heat-flow anomalies occur in the graben. These are the prime targets of geothermal energy exploration, including the deep-heat-mining project Basel (DHM Basel).

The fault pattern in the Upper Rhine Graben (URG) at this location consists of faults striking NNE, ENE and NW, related to the rift/graben structure, the Rhine-Bresse transfer zone and the Variscan orogeny, respectively. These basement fracture zones are prone to

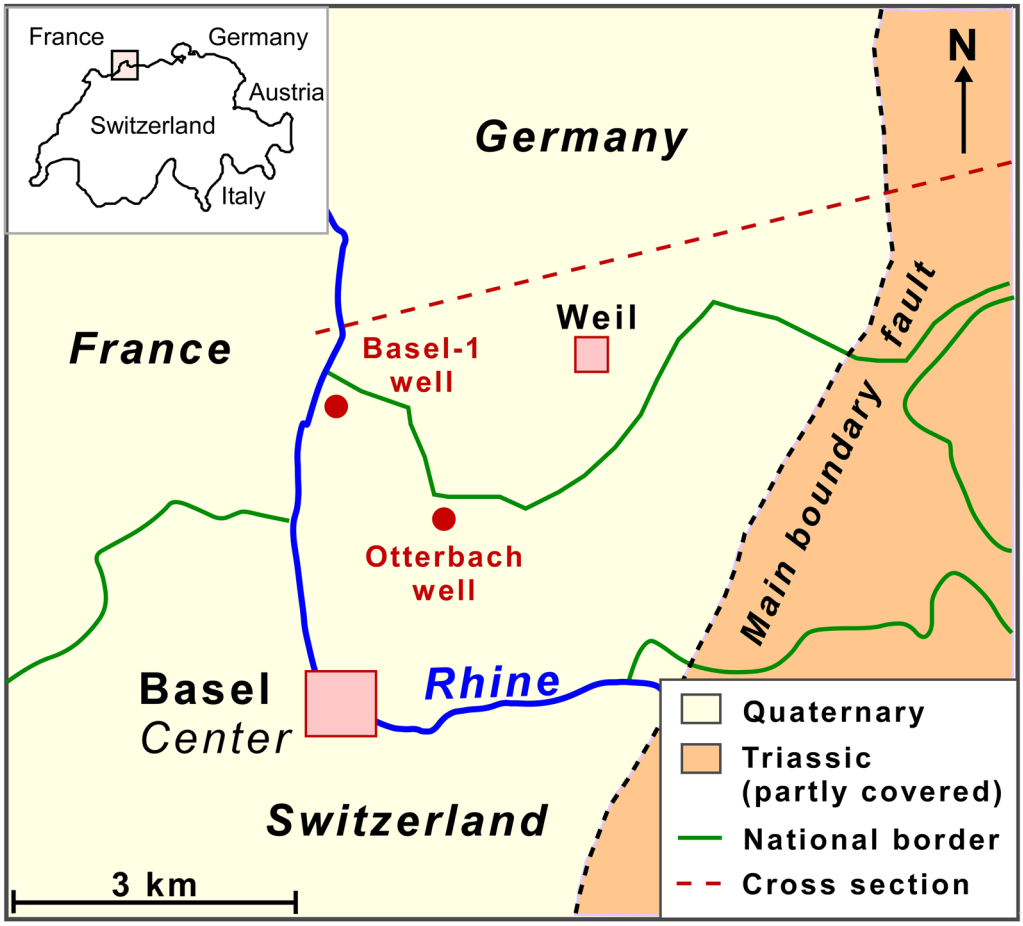


**Fig. 1** Location of the investigated borehole Basel-1 and the Otterbach well in northern Switzerland, near the river Rhine. The geological cross section is shown in Fig. 2

present-day activation by neotectonic activity (Häring, Ladner, et al., 2008; Ustazewski & Schmid, 2007).

### 2.1 Geology of the deeper part of the Basel-1 borehole

The Basel-1 borehole is approximately vertical and reaches a depth of 5000 m. The borehole passed through a 2507 m thick cover of Quaternary, Cenozoic, Mesozoic (Jurassic and Triassic), and Permian sediments before entering the crystalline basement (Fig. 2). The borehole is cased up to 4629 m depth with an open hole section from 4629 to 5000 m (Häring, Ladner, et al., 2008).

The drilled crystalline basement was formed during the Variscan orogeny and represents the continuation of the Black Forest and Vosges massifs covered by the graben sediments (see Dezayes and Lerouge (2019) and references therein for local geology). The drilled basement consists exclusively of undeformed plutonic rocks and a few lamprophyric and aplitic dykes. The rocks range from hornblende-bearing, quartz-rich biotite-granite at the top of the basement to monzogranite, monzonite and monzodiorite in deeper borehole sections (Kaeser et al., 2007). The granitoid rocks locally show different types of hydrothermal alteration: e.g. formation of albite, epidote, anhydrite, calcite, and clay minerals (Ziegler et al., 2015).

Ziegler et al. (2015) carried out a detailed analysis of natural fractures in the crystalline basement rocks of the Basel-1 well. They found, that natural fracture frequency decreased with depth from 3.1 fractures/m near the top of the basement (100 m below the weathered granite palaeo-surface) to 0.3 fractures/m below 3.0 km depth. While in the upper part of the basement fracture orientation varied, in the lower part only steeply dipping to W-SW fractures are present. Additionally, Ladner et al. (2008) describe two cataclastic fault zones in 4700 and 4835 m depth, i.e. in the open hole section. These fault zones contain strongly altered feldspar, clay minerals, and some anhydrite. The low fracture frequency in the open hole section is verified by the analysis of the drill cores at 4899.8–4908.5 m depth that contained no natural fractures.

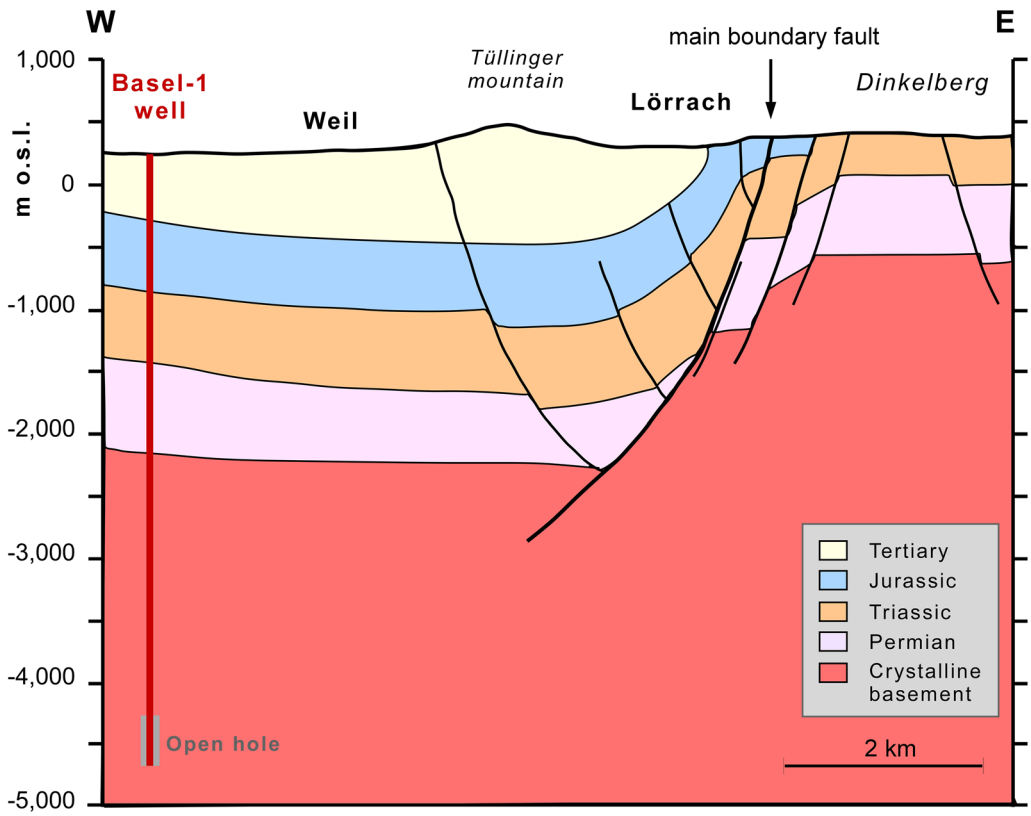


**Fig. 2** WSW-ENE cross section (see Fig. 1) north of Basel, showing the sedimentary cover and tectonic situation of the area

The hydraulic test models presented below support the geological observation that only few steep natural fractures (faults) are present. The hydraulic structure of the entire open hole section is consistent with few poorly connected local fractures.

### 2.2 Hydraulic tests in the Basel-1 well

After cleaning of the Basel-1 borehole with freshwater but before massive stimulation hydraulic tests were carried out during 23–26. November 2006. The tests were needed for developing a concept for the planned massive hydraulic stimulation of the basement rocks in the open hole (4629–5000 m depth) (Häring, Ladner, et al., 2008). The data and the derived hydraulic models from these tests directly relate to the hydraulic structure and properties of the undisturbed reservoir in the basement at 5 km depth.

During the later hydraulic experiments, carried out between 2nd and 8th December 2006, a total volume of 11,566 $m^3$ freshwater from the nearby river Rhine was injected for massive stimulation purposes into the borehole. After the massive hydraulic injections the well was shut-in for a short period. It was then decided to bleed-off the well to its natural hydraulic pressure. The bleed-off phase lasted about 4 days. Afterwards, the well was left open for free outflow (Häring et al., 2008a, b). However, during the free outflow period the water level in the borehole showed a dynamic behavior with regular fluctuations and intermittent 'blow-outs' of about 25–27 $m^3$ water each time. Thus, backflow was discontinuous. A cumulative backflow of about 3900 $m^3$ was produced until April 2009, i.e. over a 28-month period.

In January and February 2009 several low-rate injection and production tests were carried out in order to confirm the enhancement of permeability (Ladner & Häring, 2009).

### 2.3 Temperature in the open hole

Unfortunately, reservoir temperature of the Basel-1 borehole was never measured before the hydraulic stimulation activities. The first temperature-log was run in December 2008, e.g. two years after the massive hydraulic injection test (Ladner & Häring, 2009), when the borehole was still producing intermittent outflow. The temperature-log reached a depth of 4600 m and ended 29 m above the casing shoe with a temperature of 173.6 °C. A second temperature-log was run in June 2009 reaching a depth of 4682 m, i.e. it went 53 m into

the open hole and a maximum temperature of 174 °C was recorded (Ladner & Häring, 2009). The T-log in the accessible section of the open hole of Basel-1 was characterized by thermal perturbations (Ladner & Häring, 2009), most probably caused by the outflow of still colder injected water. This implies that thermal equilibrium has not been established, mainly due to the long lasting outflow at the wellhead of former injected freshwater.

A mean geothermal gradient of 4.1 °C/100 m in the sedimentary section and of 2.7 °C/100 m in the crystalline basement resulted from the logs. These are typical values for deep wells in the Moldanubikum unit of Central Europe (e.g. Agemar et al., 2013; Genter et al., 2010), where temperature increase with depth is mainly caused by rock internal heat production. The data imply that the temperature at 5 km depth is close to 183 °C. A similar temperature of 190 °C has been deduced by Ladner et al. (2008) for the depth of 5 km.

## 3 Results

### 3.1 Natural hydraulic conditions in the open hole of Basel-1

During the pre-tests, viz. before stimulation, pressure was measured at the choke manifold, i.e. at wellhead (Geothermal Explorers, 2006). At that time the borehole was filled with freshwater from the nearby river Rhine having a much lower density than the water stored in the crystalline basement and, as a consequence, the borehole showed artesian conditions. The hydraulic pre-tests (Fig. 3) are composed of two 'outflow tests' and one injection test (Häring, Ladner, et al., 2008; Ladner et al., 2008). The 'outflow tests', e.g. free outflow of freshwater of the artesian confined borehole, correspond hydraulically to pumping tests (P1, P2 Fig. 3) and are therefore in the following referred to as pumping tests. After each of the two short pumping tests pressure-recovery in the borehole was measured (shut-in, $Q = 0$ L min$^{-1}$). The injection test was carried out with three different injection rates Q (Fig. 3). Caused by injection, pressure increased from 14.8 bar up to 32.9 bar, 52.2 bar, and 73.8 bar, respectively (blue curve Fig. 3). Due to the low pumping- and injection rates with resulting relatively low pressure changes no elastic reaction of the granitoid basement or other major disturbances of the in-situ permeability are to be expected and are as well not observed during our evaluation of the pressure drawdown and -increase. Thus, the pre-tests with their observed pressure changes reflect the natural reactions of the tested granitoid rock along the open hole section resulting from the hydraulic structure of this basement.

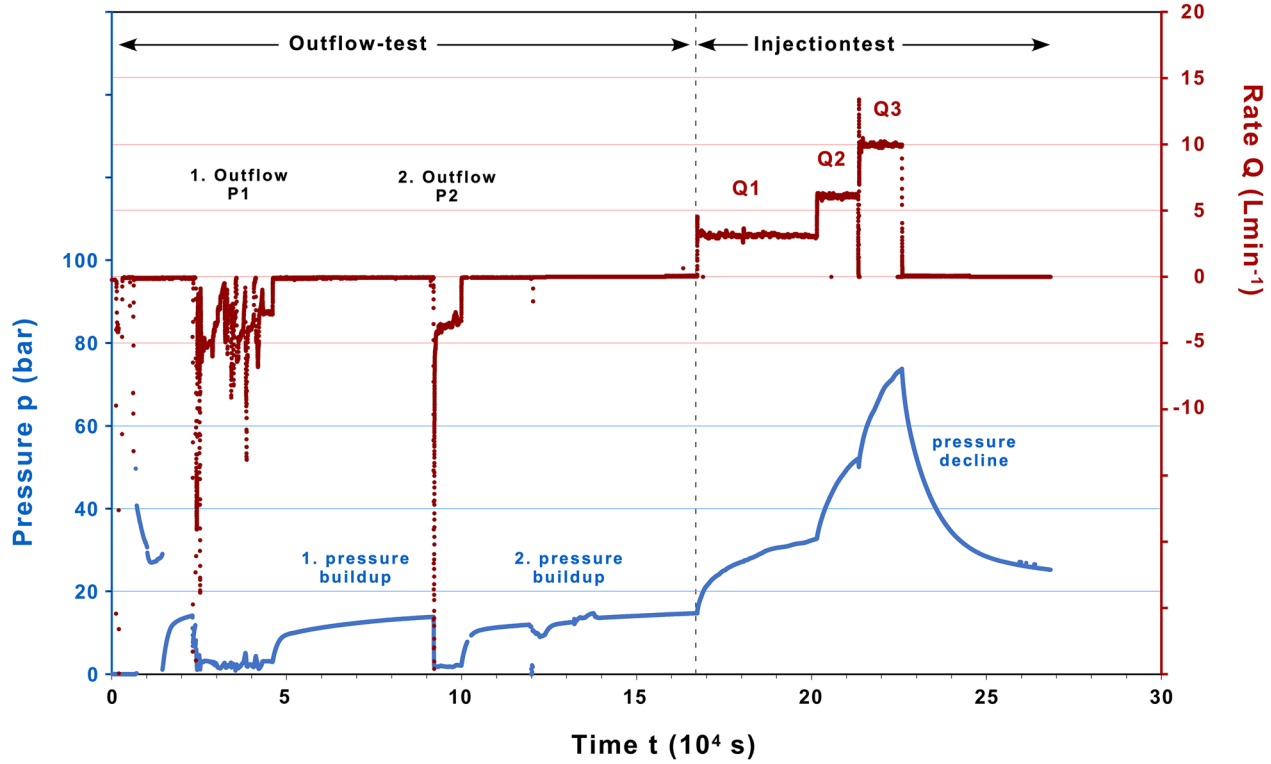


**Fig. 3** Overview of the pre-test carried out in the Basel-1 borehole. Injection rates: $Q_1 = 3.14$; $Q_2 = 6.09$; $Q_3 = 9.94$ (L min$^{-1}$)

Note: All pressures given in the study refer to hydrostatic pressure exerted by the fluid (groundwater) in the open fracture porosity of the granitoid basement (about 500 bar at 5 km depth for pure water). The lithostatic pressure at 5 km depth is close to 1.4 kbar. The pressure effect on the considered water–rock equilibria is relevant for processes in the microporosity of the basement rocks but have been ignored here because it is not the topic of the communication. The small fluid pressure increase from about 500–559 bar during the pre-tests in a setting of a high lithostatic pressure cannot cause an increase in the effective fracture porosity.

In the following we present the evaluation of the pressure increase during the first part of the injection test with a constant rate of $Q = 3.14$ L min$^{-1}$. In the first period pressure increase was dominated by a bilinear flow regime, which is recognizable as a straight line, when pressure is plotted versus the 4th root of time (e.g. Bourdet, 2002; Cinco & Samaniego, 1977; Stober, 1986) (Fig. 4b). Bilinear flow means in effect, that in the tested open-hole only few, more or less vertical fractures (or faults) take up the injected water. From these fractures (or faults) the water will be transported via micro-fractures approximately perpendicular into the granitic rock.

In the course of pre-test injection, superseding the bilinear flow regime, a radial flow regime takes over, recognizable as straight line on the pressure (p) versus logarithm of time (log t) graph (Fig. 4a). The figure shows pressure increase of the 1st injection-step (injection-rate $Q_1 = 3.14$ L min$^{-1}$). The radial flow regime is established at the end of injection (straight line Fig. 4a). From the measured pressure increase during the first injection phase with $Q = 3.14$ L min$^{-1}$ a transmissivity of $T = 7.1$ $10^{-8}$ m$^2$s$^{-1}$ can be computed (Cooper & Jacob, 1946). This transmissivity characterizes the open hole section. In contrast to the 1st injection-step ($Q_1 = 3.14$ L min$^{-1}$) the 2nd and 3rd injection-steps ($Q_2 = 6.09$ L min$^{-1}$ resp. $Q_3 = 9.94$ L min$^{-1}$) were too short and could not be evaluated separately.

Due to the short duration of the pre-stimulation pumping tests with fluctuating outflow (Fig. 3) an evaluation of the drawdown was not possible. However, the pressure recoveries after these two tests could be analyzed by using HORNER-plots (Horner, 1951) and transmissivity of the basement in the open-hole section was calculated to $T = 1.27$ $10^{-7}$ m$^2$ s$^{-1}$ for both recoveries. An equivalent evaluation was carried out for the pressure-decline after the injection test leading to a transmissivity of $T = 1.21$ $10^{-7}$ m$^2$ s$^{-1}$ (Fig. 5).

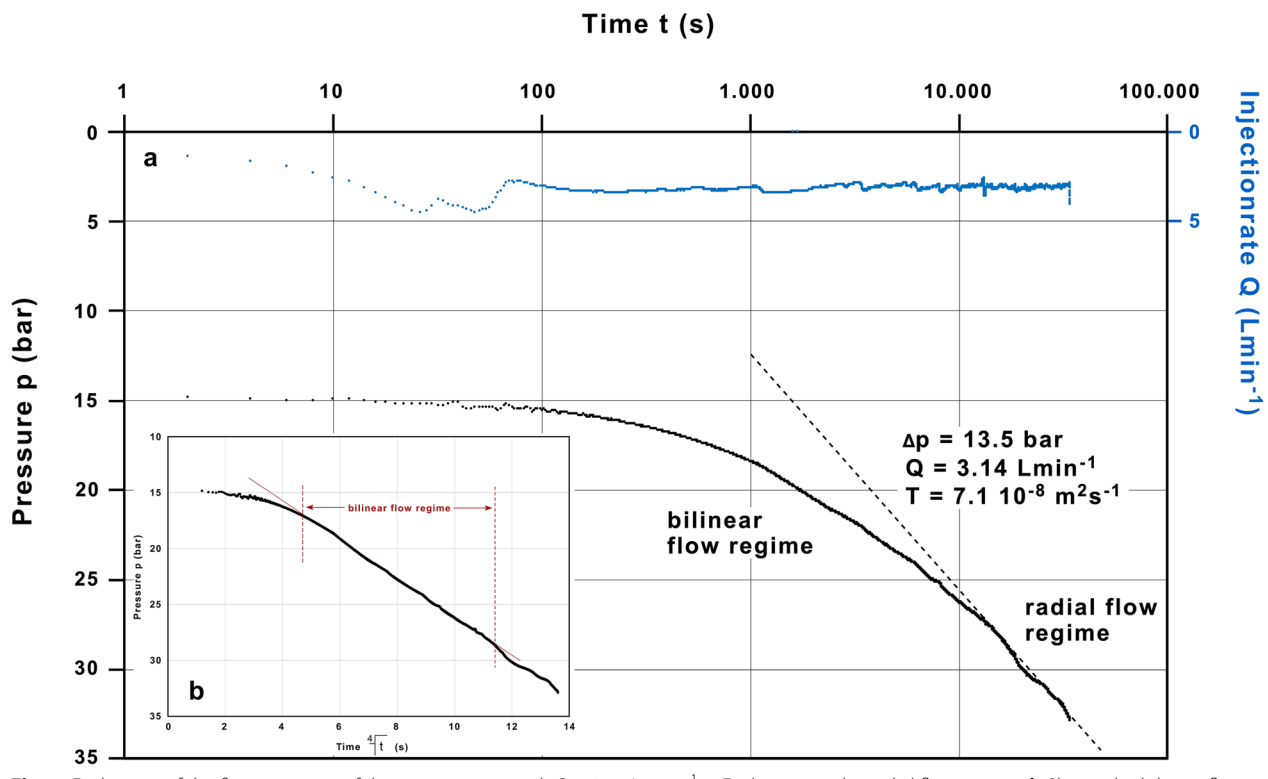


**Fig. 4** Evaluation of the first sequence of the injection test with $Q = 3.14$ L min$^{-1}$. **a** Evaluation in the radial flow regime. **b** Shows the bilinear flow regime before radial flow sets in

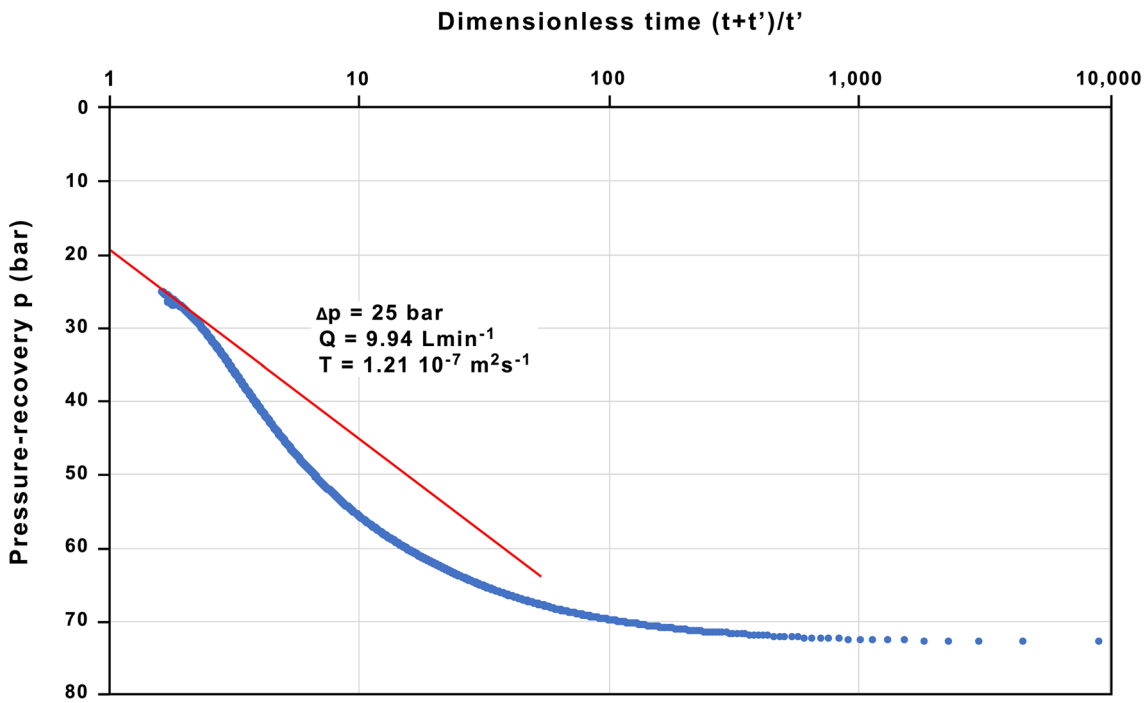


**Fig. 5** Evaluation of pressure decline after the injection test (Fig. 3) using the HORNER-plot method (Horner, 1951), with t = mean injection duration with Q = 9.94 L $min^{-1}$ (injection rate of the last injection step) and t' = recovery time

By extrapolating the measured pressure data up to the dimensionless time (t + t')/t' = 1 (Fig. 5) we determined the steady-state reservoir pressure to 19.5 bar (for freshwater in the borehole), responsible for the free outflow of the borehole. At this time the composition of outflow was still close to freshwater.

The somewhat lower transmissivity obtained from the evaluation of the pressure increase during the injection test (1st injection step, Fig. 4) in comparison to the pressure-recoveries (pumping tests, injection test) (Fig. 5) could be caused by the injection of slightly colder water into the granitoid basement in comparison to the fluid escaping from the fractures into the borehole during the pressure-recovery.

It follows from the pre-test data that the transmissivity of the open-hole section is on the order of T = 1.2 $10^{-7}$ $m^2$ $s^{-1}$ prior to the massive stimulation experiments, that is under undisturbed natural conditions. The hydraulic conductivity (K c. T/H), i.e. normalization of T versus the thickness of the open-hole section (H = 371 m), is around K = 3.2 × $10^{-10}$ $ms^{-1}$ and corresponds to a permeability of k = 5.8 × $10^{-18}$ $m^2$. The conversion K to k was done for freshwater (due to injection of river water) under reservoir conditions (500 bar, 185 °C) with the dynamic viscosity μ = 1.576 $10^{-4}$ Pa s, density ρ = 911.56 kg $m^{-3}$, and gravity g = 9.81 m $s^{-2}$ appropriate for the derived reservoir conditions.

### 3.2 Composition of water

The largest volume of the injected freshwater (11,566 $m^3$) has been taken up by the crystalline basement along the open-hole section. The storage capacity of the borehole is only about 175 $m^3$. During the dynamic outflow period a cumulative backflow of about 3900 $m^3$ from the well was recorded. Thus, by April 2009 2/3 of the injected water still remained in the fracture system of the granitoid rock.

The injected river water had a total of dissolved solids TDS = 247 mg $L^{-1}$, with calcium (Ca) and hydrogen carbonate ($HCO_3$) as main solutes (Table 1) and a pH ~ 8. A total of 12 samples of backflow water were collected and analyzed between 11. December 2006 and 5. March 2008 (Table 1). Compared with the injected freshwater, the TDS of backflow of the Basel-1 was high. The dominant solutes were Na and Cl and the pH close to neutral. TDS increased steadily from 5372 mg $L^{-1}$ to 16,697 mg $L^{-1}$ in the 16-month sampling period. However, steady state was not achieved (Table 1). The observation implies that the original fluid stored in the crystalline basement is significantly higher concentrated than the last water sample

**Table 1** Composition of water samples from the outflow of the Basel-1 borehole and from the river Rhine

| Location | Basel BS-1[a] | Basel BS-1 | Basel BS-1 | Basel BS-1[a] | Basel BS-1 | Basel BS-1 | Basel BS-1 | Basel BS-1 | Basel BS-1 | Basel BS-1[a] | Basel BS-1 | Basel BS-1 | Rhine |
|---|---|---|---|---|---|---|---|---|---|---|---|---|---|
| Date /time | 11.12.06 (16:00) | 14.12.06 (17:25) | 14.12.06 | 16.01.07 | 05.02.07 | 23.02.07 | 29.03.07 | 20.04.07 | 15.06.07 | 27.09.07 | 06.02.08 | 05.03.08 | 28.05.15 |
| Laboratory | LV | IMPG | IMPG | IMPG | IWB | IWB | IWB | IMPG | IWB | IWB | L8 | IMPG | IMPG |
| pH | – | 6.13 | 7.12 | 7.9 | 7.56 | 7.90 | – | 7.12 | 7.50 | – | – | 6.59 | 8.07 |
| EC mS/cm | – | 11.3 | 11.3 | 14.9 | 16.9 | 15.0 | – | 18.0 | 20.0 | 22.0 | – | 23.7 | 0.27 |
| Ca | 302 | 300 | 301 | 283.1 | 301 | 297 | 334 | 538 | 372 | 450 | 465 | 480 | 51.30 |
| Mg | 1.5 | 1.48 | 1.46 | 0.70 | 0.57 | 0.50 | 0.70 | 0.18 | 0.70 | 0.90 | 0.60 | 0.96 | 6.46 |
| Na | 1405 | 1981 | 1975 | 2830 | 2998 | 2940 | 3170 | 3787 | 4230 | 5360 | 5110 | 5414 | 6.57 |
| K | 175 | 207 | 207 | 294.4 | 306 | 322 | 350 | 326 | 391 | 485 | 439 | 606 | 2.40 |
| Sr | 4 | 4.9 | 4.8 | – | 6.8 | 5.9 | 7.1 | 7.6 | 9.8 | 11.7 | 11.6 | 14.1 | – |
| Rb | – | < 0.03 | < 0.03 | – | < 0.03 | – | – | 3.18 | – | – | – | < 0.03 | – |
| Li | – | 11 | 11 | 16.6 | 16 | 19.2 | 19.8 | 19.9 | 25.1 | 31.9 | 31.6 | 28.3 | – |
| Fe | – | 0.49 | 0.22 | 2.72 | 2.61 | 4.29 | 1.32 | 0.16 | 0.42 | 0.20 | – | 0.64 | – |
| Al | – | < 0.02 | < 0.02 | 0.14 | < 0.02 | < 0.01 | < 0.01 | < 0.02 | < 0.01 | < 0.01 | – | 0.04 | < 0.02 |
| As | 0.15 | 0.18 | 0.46 | 0.14 | 0.05 | 0.04 | 0.03 | 0.03 | 0.02 | 0.09 | – | 0.18 | – |
| $HCO_3$ | – | 103 | 99.5 | 141 | 140 | 133 | 138 | 125 | 45.1 | – | 117.1 | 131.2 | 145.00 |
| $SO_4$ | 782 | 605 | 598 | 311.3 | 284 | 313 | 295 | 295 | 260 | 245 | 235 | 237 | 20.50 |
| Cl | 2520 | 3598 | 3521 | 5039 | 5382 | 5410 | 5890 | 6664 | 7680 | 7980 | 8990 | 9541 | 9.44 |
| F | – | 6.0 | 5.84 | – | 5.65 | 6.00 | 5.80 | 7.89 | 5.80 | 6.20 | 6.00 | 4.97 | 0.0 |
| Br | – | 16.8 | 16.6 | – | 25.4 | 27.4 | 27.8 | 37.4 | 38.2 | 41.4 | 45.5 | 52.7 | < 0.05 |
| $SiO_2$ | 180 | 199.4 | 198.2 | – | 147.5 | 127 | 70.8 | 149 | 147 | 124.5 | 141.4 | 121.3 | – |
| $HBO_2$ | – | 25.4 | 24.6 | 34.6 | 46.3 | 51.9 | 43.4 | 45.8 | 53.5 | – | – | 64.3 | – |
| TDS | 5372 | 7060 | 6965 | 8954 | 9662 | 9658 | 10354 | 12005 | 13259 | 14737 | 15593 | 16697 | 247.07 |

Concentrations are given in mg $L^{-1}$

– not analyzed

[a] Partial analysis; Laboratories: LV Laboratory Veritas; IMPG Mineralogy Freiburg; IWB Industrielle Werke Basel; L8 (Ladner et al., 2008)

from the outflow. The data from the first sample, taken only 3 days after the end of massive hydraulic injection, indicate that the outflow water represents essentially diluted formation water in contact with the granitoid rocks.

The cations Na, Ca, K, and Li increased with time in contrast to decreasing Mg. The anions Cl and Br increased whilst $SO_4$ decreased. The concentration of $HCO_3$ and F remained constant. The major solutes and the TDS given in Table 1 are displayed graphically in Fig. 6.

Although Cl, Br, and Na increase with time, Cl/Br and Na/Cl ratios remain constant at molar Cl/Br ± 451 (mass ± 200) and Na/Cl ± 0.87. Dissolved $SiO_2$ is irregular and varies between 121 mg $L^{-1}$ and 199 mg $L^{-1}$. Molar Ca/$SO_4$ increased steadily from 0.93 up to 4.85 during the sampling period, caused by increased Ca and decreased $SO_4$ within the observation time. The mole fraction $X_{Na}$ (Na/(Na + Ca) increases in the first fluid samples from $X_{Na} = 0.89$ to $X_{Na} = 0.95$ and remains constant in the last samples.

The Na-Cl type saline outflow water (Fig. 7) has the typical hydrochemical characteristics of deep water residing in many crystalline basement complexes (e.g. Edmunds & Savage, 1991; Frape & Fritz, 1987; Pauwels et al., 1993; Stober & Bucher, 1999a; Sanjuan et al., 2016). The saline solutions are very low in Mg, low in $HCO_3$, and contain considerable $SO_4$. Remarkably, the injected river water had higher Mg than the outflow water (Fig. 7; Table 1).

### 3.3 Leaching experiments

Powders of quartz-monzodiorite (Fig. 8) from 4900 m depth were leached with deionized water at room temperature (see supplement methods). Despite the low temperature of the two experiments the powder reacted drastically with water and the TDS of the produced fluids increased from < 1 to 105 mg $L^{-1}$ (Table 2). The alkaline leachates reached pH = 9.86 in both experiments. Also, the composition of the fluids is nearly identical. It follows from the data in Table 2 that silicate hydrolysis reactions increased pH and consequently dissolved significant Al. The dissolved $CO_2$ and $HCO_3$ present in the deionized water used in the experiments provides only 12 wt.% of the carbonate species of the leachate. However, most of the total inorganic carbon has been provided by the atmosphere. Also, ion exchange reactions increased pH and alkalis in the solution. Important is the observation that considerable Cl and F was readily mobilized from the monzodiorite reservoir rock (Table 2).

## 4 Discussion

### 4.1 Hydraulic properties

Evaluation of the hydraulic pre-tests provided the hydraulic characterization of the open hole section in the reservoir rocks. The data analysis suggests that only

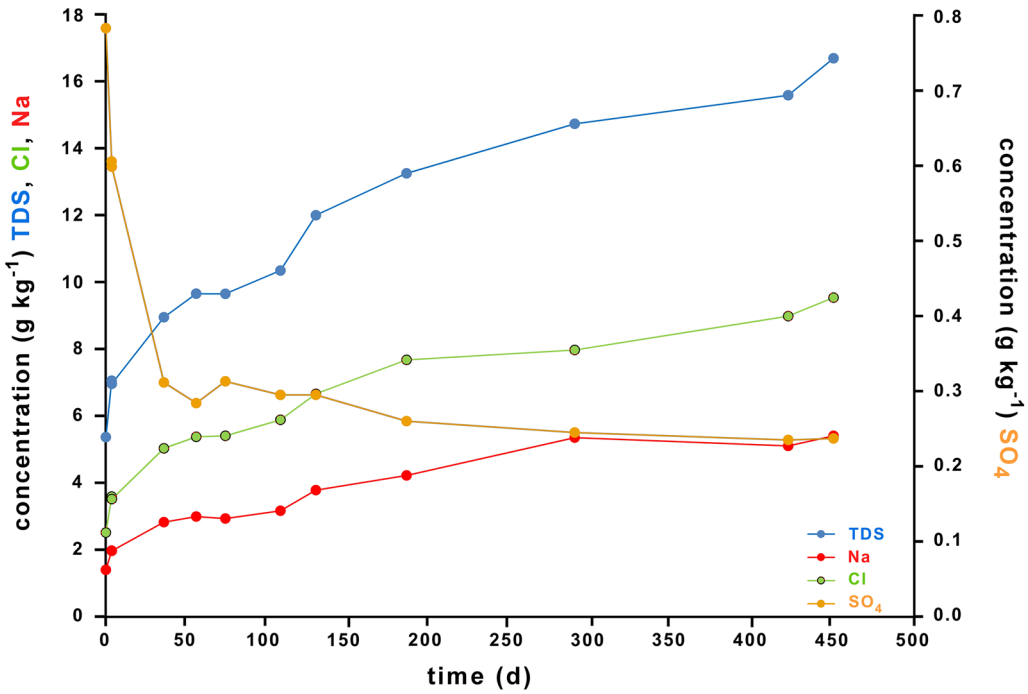


**Fig. 6** Total dissolved solids (TDS), Cl, Na, and $SO_4$ of outflow vs. sampling time (days after first sample). First water sample was taken 11th Dec. 2006

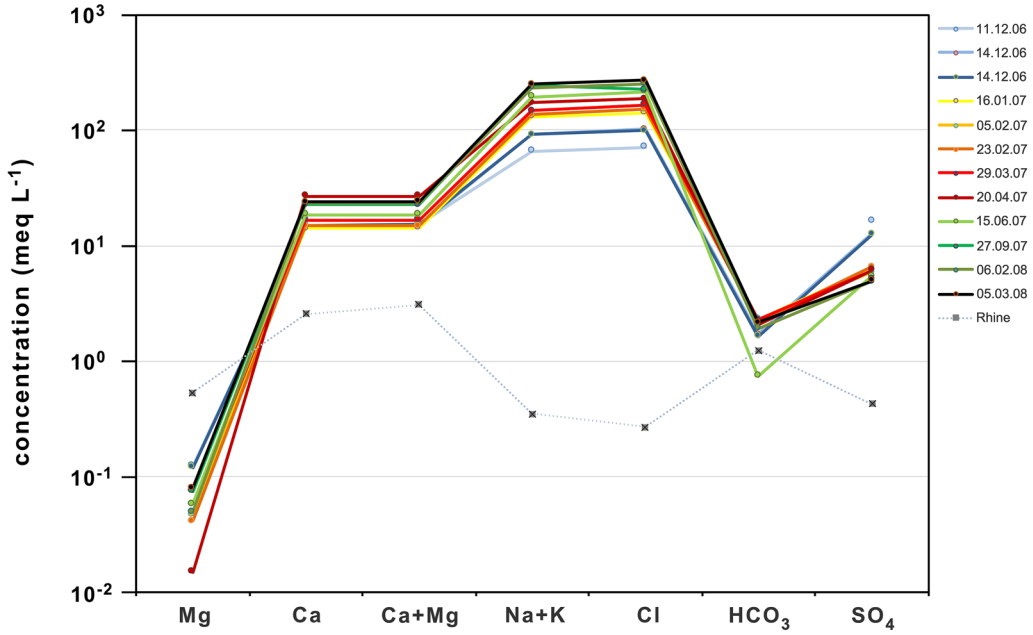


**Fig. 7** Schoeller-diagram showing the main water components of water samples of the Basel-1 outflow and of the river Rhine


**Fig. 8** Sample of quartz-monzodiorite, the predominant reservoir rock of the Basel-1 site at 4900 m depth; (width of sample ~ 3.5 cm). The coarse grained undeformed plutonic rock contains plagioclase, alkali feldspar, quartz, biotite, hornblende and accessories. Modal plagioclase ~ 55 vol.%, $X_{An}$ ~ 0.34 (rock composition given in Table 3)

few vertical fractures (faults) are hydraulically responding to water extraction and injection (bilinear flow). Further water transfer occurs via micro-fractures into the granitic rock. However, there is only insubstantial hydraulic interconnection between the dominant fractures (faults).

The derived natural hydraulic conductivity $K = 3.2 \times 10^{-10}$ ms$^{-1}$ corresponding to a permeability $k = 5.8 \times 10^{-18}$ m$^2$ of the granitic basement at 4629–5000 m depth is relatively low compared to data from granitic basement from elsewhere where typical conductivity is about one order of magnitude higher at the same depth (e.g. Manning & Ingebritsen, 1999; Stober & Bucher, 2006). Hydraulic tests in the GPK2 well at Soultz-sous-Forêts in the URG deduced a natural hydraulic conductivity of granite at 4160–5084 m depth $K = 2.2 \times 10^{-9}$ ms$^{-1}$ (Tischner et al., 2006). Also relative

**Table 2** Composition of leachate (mg L$^{-1}$)

| | | | |
|---|---|---|---|
| K | 28.0 | $CO_3$ | 22.2 |
| Na | 12.3 | $HCO_3$ | 30.0 |
| Ca | 1.5 | Cl | 5.2 |
| Mg | 0.3 | $SO_4$ | 2.0 |
| Al | 1.8 | F | 1.6 |
| | | Br | < 0.02 |
| TDS | 105.3 | pH | 9.89 |

From 30.105 g rock powder in 200 ml water

to other naturally permeable fractured reservoirs tested in deep boreholes of the central and southern URG (Vidal & Genter, 2018) the permeability of basement rocks at Basel-1 is low.

The hydraulic conductivity of the basement at the KTB-VB borehole (German deep continental drilling pilot hole) is $K = 4.07 \times 10^{-8}$ ms$^{-1}$ at 3850–4000 m depth. Testing the Urach 3 research borehole SW Germany (Eastern Black Forest gneissic basement) provided $K = 1.49 \times 10^{-9}$ ms$^{-1}$ at 3320–3488 m depth (Stober & Bucher, ). The conductivity at these sites is higher than at Basel-1, but they characterize basement rocks at shallower depths. Using the depth vs. K relationship derived from the Urach-3 basement (Stober, 2011; Stober & Bucher, 2014) the extrapolated conductivity for 5000 m depth is $< 10^{-11}$ ms$^{-1}$. Consequently, the Basel-1 granitoid basement with its coarse grained plutonic rocks has a measured natural hydraulic conductivity which is higher than the expected (extrapolated) conductivity of the Urach-3 gneissic metamorphic basement at the same depth of 5 km.

At the Basel site, in contrast to most other deep boreholes in the URG, no significant fluid circulation with up- or downward components within the basement has been detected. The temperature logs showed a nearly constant gradient of 27 °C km$^{-1}$ in the basement with no evidence for significant vertical fluid flow.

### 4.2 Salinity of the basement fluid in the Basel-1 borehole

The outflow water is a salty NaCl solution. The salt content originates from the original formation water residing at depth. This deep water has been mixed with various amounts of the river water during stimulation works and after that. Generally, the salt content of deep basement fluids is derived from both external and internal sources. External sources include fossil seawater or dissolution of halite from a (former) sedimentary cover and its infiltration into the basement. Internal sources of chloride include alteration of biotite or amphibole releasing Cl, cracked salty fluid- inclusions and of halite present on minerals grain-surfaces (e.g. Markl & Bucher, 1998; Stober & Bucher, 1999b). Once in solution chloride can be passively increased by $H_2O$-consuming mineral reactions (Stober & Bucher, 2004). A mechanism that generates saline pH-neutral waters is e.g. zeolite formation replacing feldspars binding $H_2O$ of the fluid into the structure of a framework silicate (Stober & Bucher, 1999b, 2004; Weisenberger & Bucher, 2010).

The Cl/Br ratio (mass ratio) in the fluids residing in granitoid basement is typically about Cl/Br = 100 or less (e.g. Behne, 1953; Correns, 1956), in modern seawater Cl/Br = 288 (Stumm & Morgan, 1975), and in brines from dissolved halite deposits several thousands (Stober & Bucher, 1999b). Fluid inclusions in crystalline basement rocks show very different Cl/Br ratios depending on the origin of the fluid (internal or external source) (e.g. Mullis, 1987; Yardley & Banks, 1995). Fluid inclusions have Cl/Br > 288 if derived from halite dissolution (Böhlke & Irwin, 1992). However, brittle deformation such as fracturing and faulting of granite and monzonite of the Black Forest region representing exposed basement of the URG opens up easily leachable salt with very low Cl/Br ratios (Bucher & Stober, 2002; Drüppel et al., 2020; Stober & Bucher, 1999b). The lowest Cl/Br mass ratios of leachable salt were in the range 20–50. This explains the typically low Cl/Br ratio of saline deep groundwater in basement rocks (Bucher & Stober, 2002).

The NaCl-rich formation water of the basement at Basel-1 (TDS > 16,697 mg L$^{-1}$) has been diluted with a NaCl-poor river water (TDS = 247 mg L$^{-1}$) during stimulation injection. Therefore, the Cl/Br ratio of the diluted basement water remains constant and reflects the Cl/Br of original formation fluid residing at depth.

The observed constant Na/Cl ratio suggests that the alteration reactions involving primary Na-bearing silicates did not alter the bulk fluid notably. While the Na/Cl ratio of modern seawater is Na/Cl = 0.86 (mol ratio), that of dissolved halite is Na/Cl = 1.0. The Na/Cl ratio of the outflow indicates that the fluid salinity is not derived from halite dissolution.

The measured Cl/Br ratio of the outflow is significantly lower than that of modern seawater and orders of magnitude lower than that of dissolved evaporitic salt. It follows from the constant Na/Cl ratio and the enhanced Cl/Br ratio (Cl/Br ± 200) that the salinity of the outflow has a significant seawater component, but no halite signature. Additionally, the Cl/Br ratio of the outflow water (lower than seawater) is typical for fluids that have interacted with basement rocks. The Na/Cl ratio of water also depends on the mineral assemblage of the rock, especially on the composition of plagioclase ($X_{An}$) (Orville, 1972; Stober & Bucher, 2005) in addition to a possible imported seawater component. Interaction with plagioclase results in a temperature dependent Na-Ca signature of the fluid. The andesine (plagioclase $X_{An} = 0.34$) present in the Qtz-monzonite controls Na/Cl to distinctly below < 0.86 at 200 °C. Consequently, direct plagioclase dissolution did not significantly contribute to the observed Na/Cl of the outflow. A similar conclusion has been drawn from computed fluid evolution models for the Basel-1 site (Alt-Epping et al., 2013).

The high salinity of the outflow and the expected even higher salinity of the undisturbed formation water suggests that the hydration of primary igneous monzodiorite fixed $H_2O$. Kaeser et al. (2007) report medium to high

salinities in fluid inclusions found in different minerals of the reservoir rock. The leaching experiments produced 34 mg $L^{-1}$ chloride per kg rock and L of water (Table 2). Thus, the monzodiorite represents an internal Cl source for salinity of the reservoir fluid. The molar ratio Na/Cl = 3.6 in the leachates suggests that the salinity of the formation water in the monzodiorite is additionally externally (seawater) derived. The Na/Cl ratio (mol ratio) in the leachate indicates that much of Na is originated by ion exchange from the surface of plagioclase ($Na^+$-$H^+$). Origin of $SO_4$ in the leachate is caused by oxidation of pyrite.

The composition of leachates (Table 2) shows that pure water–rock interaction (WRI) produces "basement" water with high pH, high molar Na/Cl ratios and low TDS. The produced fluid is an alkali-chloride-carbonate solution. The total inorganic carbon mostly originates from the atmospheric $CO_2$ including $CO_2$ in the deionized lab water. Thus, the remaining WRI produces a low TDS Na–K-$HCO_3$-Cl water with a pH close to 10. This corresponds to very similar natural WRI water in the Gotthard basement collected in the NEAT rail base tunnel at depth of up to 2700 m (Bucher et al., 2012; Stober et al., 2022).

The TDS of the undisturbed reservoir fluid at 5 km depth and ~ 200 °C is a parameter of prime interest. However, it is difficult to access from extrapolation of the outflow data. The TDS of the fluid at the Soultz-sous-Forêts site in the URG is about 100 g $kg^{-1}$ (Genter et al., 2010; Sanjuan et al., 2016).

Still, the predrilling TDS of the reservoir fluid can be deduced from the evaluation of hydraulic data. From the hydraulic data presented above follows a steady-state reservoir pressure of 19.5 bar for freshwater in the borehole. Before cleaning and filling the borehole with river water the well did not show artesian conditions, i.e. water table in the borehole was below surface. However, the static water level in the borehole was never measured. The water table monitoring station is installed at 35 m b.s. in the well and it was expected that the water table would not decrease to below this depth. In Ladner et al. (2008) a water table of at least 15 m below surface is documented, similar to the nearby Otterbach well (Fig. 1). It follows that the static predrilling water table in the Basel-1 borehole was between below 15 and considerably above 35 m b.s. A water with a TDS of ~ 45 g $kg^{-1}$ has about the same total weight and thus exerts the same pressure as the water column of freshwater with an 'over-pressure' of 19.5 bar. It follows that the average TDS of the reservoir fluid was about 45 g $kg^{-1}$.

### 4.3 Chemical effects of freshwater injection

Some solutes of the outflow increase during the 14-month sampling period while others e.g. $SO_4$ decrease or remain approximately constant e.g. F (Table 1). The injected river water contains Mg = 6.5 mg $L^{-1}$ whilst Mg in the outflow fluid is only about 1 mg $L^{-1}$ (Table 1). This suggests—ignoring ongoing new WRI-reactions—that the outflow represents a mixture of about 1 volume river water and 5 volumes of formation water.

The pH in the outflow varied between 6.1 in very first sample and 7.9 and is lower than in the injected freshwater (Table 1).

The chemical interaction of freshwater with the reservoir rock did not contribute significantly to the bulk composition of the outflow because of slow kinetics of silicate reactions. However, reactions involving accessory sulfides of the quartz-monzodiorite and the oxygen-rich river water produced initially sulfate that later returned to the original background concentration (Fig. 6). The freshwater injection created an oxydation front that propagated from the open hole into the reservoir rock. This process has been quantitatively modeld by Alt-Epping et al. (2013) for the case that the saline formation water residing in the fracture space can be ignored.

Since hydraulic conductivity of the reservoir rock is very low and restricted to a few open fractures the massive hydraulic injection of freshwater displaced the original reservoir fluid along the main fractures into small fissures intersecting the main fractures (bilinear flow). Consequently, mostly freshwater was present during injection on fractures closer to the well and interacted with the reservoir rocks. The injected oxygen-rich freshwater creates an oxidation front in the reservoir and the surface-water, containing also $CO_2$, promotes alteration reactions. Immediately, after the injection, i.e. during the bleeding-off and the shut-in, the former 'displaced' original reservoir fluid starts to flow back into and along the main fractures, leading to enhanced mixing with the partly reacted 'freshwater'.

The conservative components Cl and Br are not involved in alteration reactions. Increasing Cl and Br in the outflow reflects the decreasing fraction of river water present in the outflow and the effect of the general desiccation process.

The fluid at depth always is in contact with quartz. Thus, dissolved silica in the Basel-1 outflow depends on

the temperature dependent solubility of quartz and the river water—formation water ratio.

Origin of $SO_4$ in the outflow water is caused by oxidation of pyrite (Eq. 1). Sulphate is highest at the beginning of the sampling period and decreases with time because oxygen is gradually used up in this process. The presence of pyrite has been documented by Kaeser et al. (2007).

$$2\,FeS_2 + 7\,H_2O + 7.5\,O_2 = Fe(OH)_3 + 4\,SO_4^{2-} + 8\,H^+. \quad (1)$$

The reaction produces goethite or schwertmannite or other Fe(III) oxyhydrates or oxyhydratesulphates in the basement rock decreasing pH of the outflow water. The first outflow water sample had the highest $SO_4$ content and the lowest pH (Table 1).

Kaeser et al. (2007) described the presence of anhydrite ($CaSO_4$) on cutting material of the basement rocks in the open hole section in veins and fractures. Ladner et al. (2008) also found anhydrite in the two fault zones of the open hole. Anhydrite is not present in the rock matrix (Hofer, 2015). Thus, anhydrite is a deposition in water conducting fractures during predrilling fluid-rock interaction in the reservoir. Outflow water is generally supersaturated with respect to anhydrite and the saturation index $SI_{Anh}$ decreases with time from $SI_{Anh} = 0.91$ to $SI_{Anh} = 0.25$ for subsurface conditions (~ 180 °C) (Fig. 9). The saturation state of anhydrite is independent of pH. The described and observed anhydrite appears to be a fracture mineral precipitated from sulfate-rich fluids from predrilling processes. However, the outflow fluids tend to precipitate anhydrite on fractures rather than to dissolve it.

### 4.4 Predrilling reservoir temperature

The composition of the fluid present in the fracture porosity of basement rocks tends to progress towards chemical equilibrium with the mineral assemblage of the reservoir rock. The equilibrium fluid composition is unique for the reservoir rock and the prevailing temperature. Therefore, the reservoir temperature can be deduced from the fluid composition by geothermometry, if the type of rock dominating the reservoir is known and the system fluid-rock is at equilibrium. In the following we attempt to deduce the predrilling reservoir temperature at 5 km depth from reconstructed composition of the reservoir fluid. However, the undisturbed reservoir fluid was not in full overall chemical equilibrium with the igneous Qtz-monzodiorite. Thus, further postulations must be put forward for deriving meaningful hydrochemical temperatures: (a) the element ratios of solutes in the predrilling fluid reflects a metastable equilibrium at the reservoir temperature, and (b) the solubility of simple solids e.g. quartz dictates the presence of the component in the fluid and reflects partial equilibrium with the rock.

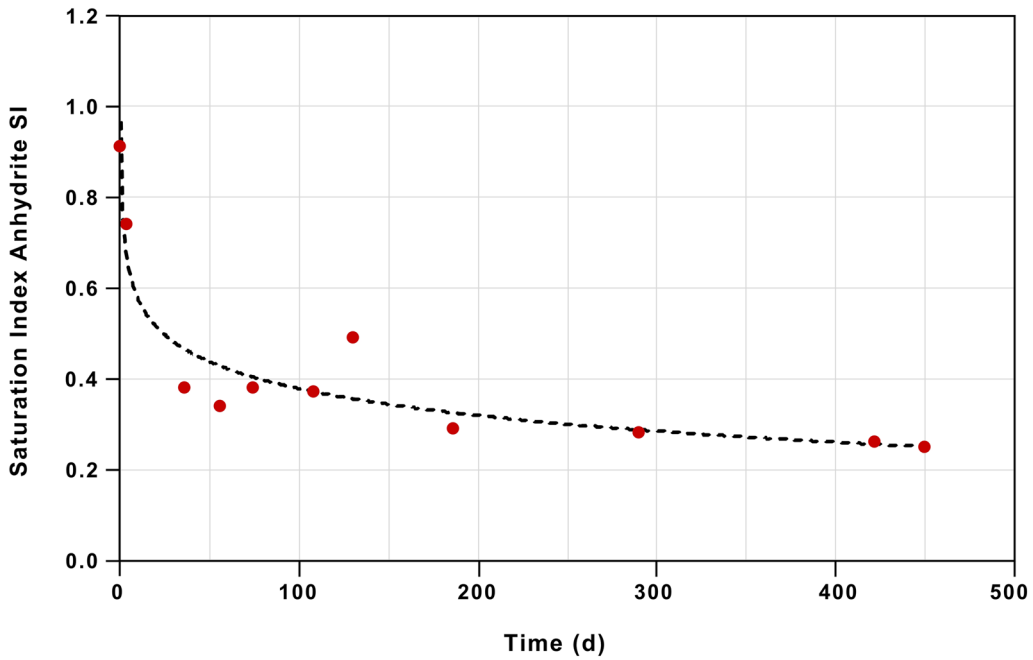


**Fig. 9** Saturation state of the outflow water with respect to anhydrite at reservoir conditions (T = 170 °C) during the sampling period

### 4.5 Solubility of quartz $SiO_2$

The pH of the outflow implies that dissolved $SiO_2$ is predominantly present as uncharged neutral complex. Because of the dilution of the reservoir fluid with injected river water the maximum-recorded dissolved $SiO_2$ corresponds to the solubility of quartz at a minimum temperature that can be computed from Eq. (2) (Stober & Bucher, 2021).

$$T = \{1114.4/(4.76713 - \log c_{SiO2})\} - 273, \quad (2)$$

where T is the temperature in °C and $c_{SiO2}$ denotes the silica concentration in mg $L^{-1}$ $SiO_2$.

During the sampling period measured dissolved silica varied between 121 mg $L^{-1}$ and 199 mg $L^{-1}$ $SiO_2$ (Table 1; Fig. 6). The resulting minimum reservoir temperature using Eq. (2) is 178 °C.

### 4.6 Temperature from the K/Na cation ratio

Although hot groundwater at depths of some km is not in full chemical equilibrium with the primary minerals of granitoid basement Na/K ratios of this water is dictated by the presence of two primary feldspars (Eq. 3).

$$KAlSi_3O_8 + Na^+(\text{fluid}) = NaAlSi_3O_8 + K^+(\text{fluid}), \quad (3)$$

Generally, the Na/K thermometer is an excellent and robust tool for deriving T-estimates from hot water residing in granitic reservoirs. Because it is based on a cation ratio dilution of the deep high-TDS water with near surface water does not usually alter the Na/K ratio of the fluid. Furthermore, the outflow does not loose preferentially K or Na to precipitating alteration minerals during the short sampling period. Our T-estimate requires the assemblage microcline (low-T K-feldspar, Kfs) and albite (Ab) and is based on Eq. (4) (Stober & Bucher, 2021).

$$T = \{-1216.7/(\log(c_K/c_{Na}) - 1.42125)\} - 273, \quad (4)$$

where T is the temperature in °C and $c_K$ and $c_{Na}$ denote the K- and Na concentration in mg $L^{-1}$ (Table 1). If the Na–K exchange reaction involves a more general alkali feldspar and plagioclase (oligoclase, andesine), the K/Na geothermometer must be modified and include a term for the activities of the components albite and K-feldspar ($a_{Ab}$, $a_{Kfs}$) in the feldspars (Stober & Bucher, 2021):

$$T = \{-1216.7/((\log(c_{K+}/c_{Na+}) + (\log(a_{Ab}/a_{Kfs})) - 1.42125)\} - 273. \quad (5)$$

In an ideal solid solution, the activity is simply equal to the mol-fraction. The mean measured compositions (Hofer, 2015) for K-feldspar results in $a_{Kfs} = 0.95$ and for plagioclase $a_{Ab} = 0.65$ in Qtz-monzodiorite using a standard state of pure microcline and pure albite at *P–T*.

During the sampling period both Na and K increased in the outflow. The Na/K ratio increased from Na/K = 9.57 (mass ratio) in early samples to Na/K = 11.64 (mass ratio) in the later samples. The calculated temperature of the geothermal fluid in the open hole section varies between 201 °C for the early samples and 186 °C for the later samples using Eq. (5). This is in excellent agreement with the measured (174 °C at 4686 m) and extrapolated temperature of 180–190 °C at 5000 m in the open hole section.

### 4.7 Mg/K temperatures

A characteristic assemblage of granitoid basement rock altered at about 200 °C is phengite (K white mica, muscovite) and chlorite (Bucher & Grapes, 2011). At temperatures below 200 °C phengite occurs as a component in clay, specifically smectite. Primary biotite contains Mg and Fe and transfers the two components to chlorite upon alteration. The content of Mg and K in deep geothermal fluid is controlled by the minerals muscovite (Ms), chlorite (Chl), and K-feldspar (Kfs) (Eq. 6).

$$\begin{aligned} &8\ KAl_3Si_3O_{10}(OH)_2 \\ &+\ 2\ Mg_5Al_2Si_3O_{10}(OH)_8 \\ &+\ 54\ SiO_2 + 20\ K^+ \\ &= 28\ KAlSi_3O_8 + 10\ Mg^{2+} + 16\ H_2O. \end{aligned} \quad (6)$$

For pure solid phases (Ms: $KAl_3Si_3O_{10}(OH)_2$; Chl: $Mg_5Al_2Si_3O_{10}(OH)_8$); Kfs: $KAlSi_3O_8$ the temperature dependence can be expressed with Eq. (7). With the activity contribution of Ms, Chl, and Kfs (Table 3) considered from Eq. (8) (Stober & Bucher, 2021) using a standard state of pure phase at *P–T:*

$$T = 34853/\left(\left(10 \log c_{Mg} - 20 \log c_K\right) + 134.51\right) - 273. \quad (7)$$

$$T = 34853/\left(\left(10 \log c_{Mg} - 20 \log c_K + 28 \log a_{Kfs} - 2 \log a_{Chl} - 8 \log a_{Ms}\right) + 134.51\right) - 273. \quad (8)$$

Temperatures derived from the Mg/K thermometer are subject to many concerns. Sources of error include e.g. unknown mineral compositions, inadequate activity model (particularly problematic for Chl) and more. The most important source of error is probably the very low concentration of dissolved Mg in many geothermal fluids. Deep fluids often contain less than 1 mg $L^{-1}$ Mg. This low Mg content presents a serious source of error. It is susceptible to analytical errors. Typical detection limits for Mg in water are about 20 µg $L^{-1}$ in standard

**Table 3** Composition of rock and minerals of Qz-monzodiorite in the open hole section of Basel-1

| | Rock | Plag | Kfs | Ab[b] | Bt | Hbl | Chl | Pump | Prh | Ms |
|---|---|---|---|---|---|---|---|---|---|---|
| $SiO_2$ | 63.32 | 60.43 | 64.09 | 66.12 | 36.95 | 50.41 | 28.86 | 37.70 | 43.66 | 48.05 |
| $TiO_2$ | 0.77 | | | | 2.71 | 0.42 | 0.14 | 0.13 | – | 0.02 |
| $Al_2O_3$ | 17.34 | 25.45 | 18.49 | 22.05 | 14.40 | 4.07 | 16.06 | 26.43 | 24.26 | 37.58 |
| FeO[a] | 4.12 | 0.08 | | | 20.65 | 15.66 | 25.73 | 3.56 | 0.13 | 0.60 |
| MnO | 0.07 | | | | 0.28 | 0.48 | 0.36 | 0.05 | – | 0.05 |
| MgO | 2.30 | | | | 11.62 | 13.49 | 16.08 | 2.04 | – | 0.21 |
| CaO | 4.23 | 7.21 | 0.01 | 1.99 | 0.36 | 12.83 | 0.16 | 24.40 | 28.30 | 0.07 |
| $Na_2O$ | 3.99 | 7.51 | 0.37 | 10.08 | 0.11 | 0.58 | – | 0.09 | 0.08 | 0.20 |
| $K_2O$ | 3.24 | 0.27 | 16.47 | 0.52 | 8.89 | 0.33 | – | 0.05 | 0.02 | 10.90 |
| F | | | | | 0.63 | 0.41 | 0.12 | 0.28 | 0.02 | 0.03 |
| Total | | | | | 96.60 | 98.68 | 87.51 | 94.73 | 96.47 | 97.71 |
| $-O\equiv F$ | | | | | 0.27 | 0.17 | 0.05 | 0.12 | 0.01 | 0.01 |
| total | 99.38 | 100.95 | 99.43 | 100.76 | 96.33 | 98.51 | 87.46 | 94.61 | 96.46 | 97.70 |
| #Ions[c] | | 8 | 8 | 8 | 11 | 23 | 14 | 12 | 12 | 11 |
| Si | | 2.669 | 2.985 | 2.883 | 2.795 | 7.365 | 3.050 | 2.965 | 2.987 | 3.096 |
| Ti | | | | | 0.154 | 0.046 | 0.011 | 0.008 | 0.000 | 0.001 |
| Al | | 1.325 | 1.015 | 1.134 | 1.284 | 0.701 | 2.001 | 2.451 | 1.957 | 2.855 |
| Fe | | 0.003 | | 0.000 | 1.306 | 1.913 | 2.274 | 0.234 | 0.007 | 0.032 |
| Mn | | | | | 0.018 | 0.059 | 0.032 | 0.003 | | 0.003 |
| Mg | | | | | 1.310 | 2.937 | 2.532 | 0.239 | | 0.020 |
| Ca | | 0.341 | | 0.093 | 0.029 | 2.009 | 0.018 | 2.057 | 2.075 | 0.005 |
| Na | | 0.643 | 0.033 | 0.852 | 0.016 | 0.164 | | 0.014 | 0.011 | 0.025 |
| K | | 0.015 | 0.979 | 0.029 | 0.858 | 0.062 | | 0.005 | 0.002 | 0.896 |
| Sum | | 4.996 | 5.012 | 4.991 | 7.770 | 15.256 | 9.918 | 7.976 | 7.039 | 6.933 |
| F | | | | | 0.151 | 0.189 | 0.040 | 0.070 | 0.004 | 0.006 |
| $X_{Fe}$ | | | | | 0.50 | 0.39 | 0.47 | | | 0.62 |
| $X_{An}$ | | 0.34 | | 0.095 | | | | | | |
| $X_{Or}$ | | 0.015 | 0.967 | 0.03 | | | | | | |

Abbreviations of mineral names Whitney and Evans (2010)

[a] All Fe as FeO

[b] Secondary albite

[c] Number of ions per number of oxygen listed

laboratories. Consequently, Mg in geothermal waters is frequently close to the detection limit.

We used the mean mol-fraction measured for microcline (0.95), clinochlore (0.50), and muscovite (0.95) (Table 3) as approximation for the respective activities in feldspar, chlorite and white mica and calculated K/Mg temperatures from Eq. (6). The calculated temperatures from both equations (Eqs. 5, 6) are very close. However, the calculated temperatures do not reach a steady state in the course of the sampling period. They increase up to a temperature of 169 °C at the end of the sampling period (Fig. 10). The pattern suggests that the derived Mg/K temperatures continue to increase somewhat. The measured /extrapolated temperature in the open hole is between 180 °C and 190 °C.

## 5 Conclusions

The hydraulic, hydrochemical, and petrological research in the open hole section of the 5 km deep geothermal well Basel-1 into Qz-monzodiorite basement has been used to evaluate the undisturbed natural conditions in the basement reservoir.

The quantitative evaluation and modeling of hydraulic pre-test data showed that only few, very steep or vertically oriented fractures (faults) are hydraulically responding to water extraction and/or injection. Thus, during later injection (massive hydraulic stimulation) the reservoir fluid was displaced along the main fractures to regions farther away from the borehole and into small fissures intersecting the main fractures.

Natural permeability of the open hole section is $k = 5.8 \times 10^{-18}$ m$^2$. This low basement permeability is

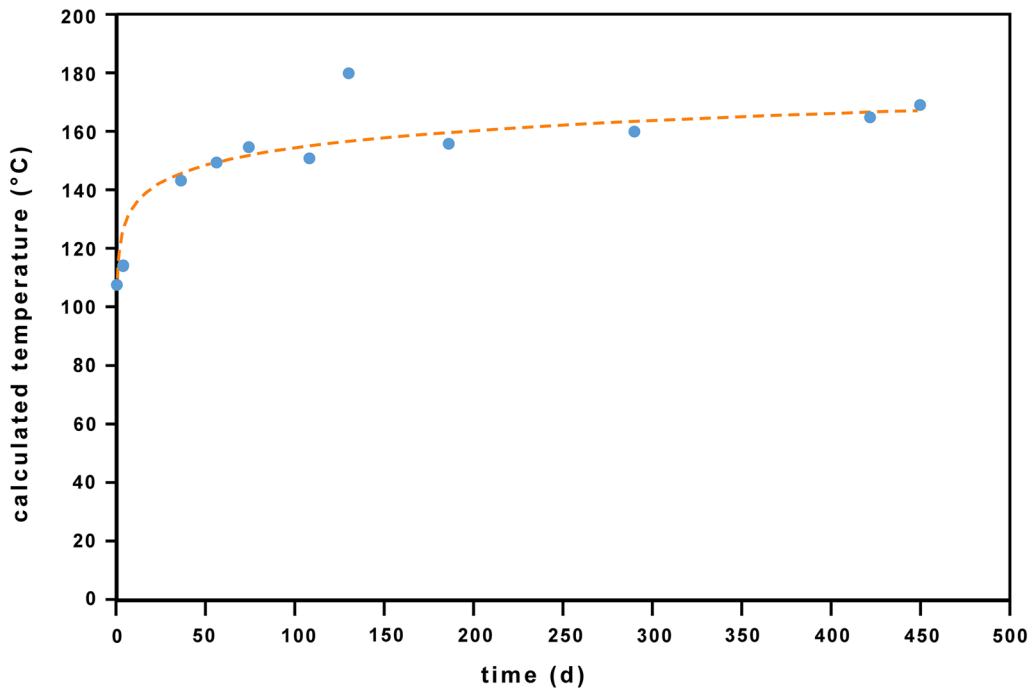


**Fig. 10** Temperatures derived from the Mg–K-geothermometer vs. sampling time (days after first sample). First water sample was taken 11th Dec. 2006. Ideal solid-solution of the endmember components in K-feldspar (95 mol%), white mica (95 mol%) and chlorite (50 mol%) (Eq. 8). For complete alteration assemblage see Table 3

plausible and expectable if compared with other data from crystalline basement at the same depth.

Since undisturbed original reservoir fluids were not sampled, the hydrochemical analysis refers to outflow water samples taken after the massive hydraulic stimulation with river water. The last collected outflow water sample had 17 g $kg^{-1}$ TDS. The hydraulic structure of the Basel-1 well implies that the TDS of the reservoir fluid is close to 45 g $kg^{-1}$. The main solutes are Na and Cl. The high TDS of the NaCl water at 5 km depth implies that it is predominantly an imported fluid with a component contributed by local fluid-rock interaction (e.g. ion-exchange, dissolution of silicates, cracked fluid inclusions). The uniform molar Na/Cl ratio of 0.86 measured in the outflow points toward to a marine origin of the salinity. The Cl/Br molar ratio of about 200 suggests that the seawater has been modified by chemical interaction with the basement rocks, whereby the seawater component is in the order of 60%. Injection of river water during the stimulation of the geothermal reservoir triggered additional new alteration processes leading, inter alia, to decreasing $SO_4$ and Mg concentrations in the outflow water in the course of the sampling period. Additional $SO_4$ is contributed by pyrite oxidation and is decreasing during the sampling period due to oxygen consumption and precipitation of late anhydrite.

The undisturbed reservoir temperature was estimated from three newly calibrated fluid geothermometers ($SiO_2$, K/Na, Mg/K). The derived hydrochemical temperatures (178 °C and 186 °C) are in excellent agreement with extrapolated temperature from T-logs (180–190 °C) in the open hole section of the borehole. The coincidence of the derived temperatures from the fluid geothermometers with T-log temperatures suggests that partial metastable equilibrium is rapidly established among fluid and the minerals of the reservoir rock at about 200 °C. The findings imply that K-feldspar and andesine (plagioclase) efficiently have power over the Na/K ratio of the fluid and the alteration assemblage Chl-Kfs-Ms present on the fracture surfaces efficiently controls the K/Mg ratio.

## Supplementary Information

The online version contains supplementary material available at https://doi.org/10.1186/s00015-021-00403-8.

**Additional file 1.** Additional material: Methods.

**Acknowledgements**
Rock samples of the Basel-1 borehole from the open hole section and raw data of hydraulic tests provided by Geothermal Explores Ltd. (Pratteln, Switzerland) is gratefully acknowledged. We are grateful to Isolde Schmidt for XRF analyses, to Sigrid Hirth-Walther for hydrochemical analyses. We are indebted to an anonymous reviewer for providing a very detailed, constructive and helpful evaluation of our submitted manuscript. We also thank the SJGS editors for the competent editorial handling of the paper.

**Authors' contributions**
IS carried out fieldwork, analyzed and interpreted the hydraulic tests and hydrochemical data, drafted the figures, tables, and the manuscript. MH carried out fieldwork and analyzed geochemical and mineralogical data. FL carried out fieldwork, assembled chemical data, and provided the hydraulic test data. KB analyzed and interpreted geochemical data and prepared the revised version of the manuscript. IS and KB approved the final submission. All authors read and approved the final manuscript.

**Funding**
Open Access funding enabled and organized by Projekt DEAL. No funding.

**Availability of data and materials**
All relevant data generated or analyzed during this study are included in this published article. Additional data are available from the corresponding author on reasonable request.

## Declarations

**Ethics approval and consent to participate**
Not applicable.

**Consent for publication**
All authors have given their consent for publication.

**Competing interests**
The authors declare that they have no competing interests.

**Author details**
[1]Institute of Earth and Environmental Sciences, University of Freiburg, Albertstr. 23b, D-79104 Freiburg, Germany. [2]Geotest AG, Freilager-Platz 3, 4142 Münchenstein, Switzerland.

Received: 28 May 2021 Accepted: 19 December 2021
Published online: 31 January 2022

**References**

Achtziger-Zupancic, P., Loew, S., & Mariéthoz, G. (2017). A new global database to improve predictions of permeability distribution in crystalline rocks at site scale. *Journal of Geophysical Research Solid Earth, 122*, 1876–1899. https://doi.org/10.1002/2017JB014106

Agemar, T., Brunken, J., Jodocy, M., Schellschmidt, R., Schulz, R., & Stober, I. (2013). Untergrundtemperaturen in Baden-Württemberg. *Zeitschrift Der Deutschen Gesellschaft Für Geowissenschaften, 164*(1), 49–62. https://doi.org/10.1127/1860-1804/2013/0010

Alt-Epping, P., Diamond, L., Häring, M., Ladner, F., & Meier, D. (2013). Prediction of water–rock interaction and porosity evolution in a granitoid-hosted enhanced geothermal system, using constraints from the 5 km Basel-1 well. *Applied Geochemistry, 38*, 121–133.

Aquilina, L., Pauwels, H., Center, A., & Fouillac, C. (1997a). Water-rock interaction processes in the Triassic sandstone and the granitic basement of the Rhine Graben: Geochemical investigation of a geothermal reservoir. *Geochimica Et Cosmochimica Acta, 61*, 4281–4295.

Aquilina, L., Sureau, J. F., & Steinberg, M. (1997b). Comparison of surface-, aquifer- and pore-waters from a Mesozoic basin and its underlying Palaeozoic basement, southeast France: Chemical evolution of waters and relationships between aquifers. *Chemical Geology, 138*, 185–209.

Banks, D., Odling, N. E., Skarphagen, H., & Rohr-Trop, E. (1996). Permeability and stress in crystalline rocks. *Terra Nova, 8*, 223–235.

Behne, W. (1953). Untersuchungen zur Geochemie des Chlor und Brom. *Geochimica Cosmochimica Acta, 3*, 186–214.

Böhlke, J. K., & Irwin, J. J. (1992). Laser microprobe analyses of Cl, Br, I, and K in fluid inclusions: Implications for sources of salinity in some ancient hydrothermal fluids. *Geochemica Et Cosmochemica Acta, 56*, 203–225.

Bourdet, D. (2002). Well test analysis: the use of advanced interpretation models. In Cubitt, J. (ed.), *Handbook of Petroleum Exploration and Production 3*, Amsterdam: Elsevier Science B.V. ISBN 0-444-50968-2.

Bucher, K., & Grapes, R. (2011). *Petrogenesis of metamorphic rocks* (8th ed.). Springer.

Bucher, K., & Stober, I. (2002). Water–rock reaction experiments with Black Forest gneiss and granite. In I. Stober & K. Bucher (Eds.), *Water–rock interaction* (pp. 61–95). KLUWER Academic Publishers.

Bucher, K., & Stober, I. (2010). Fluids in the upper continental crust. *Geofluids, 10*, 241–253.

Bucher, K., Stober, I., & Seelig, U. (2012). Water deep inside the mountains: Unique water samples from the Gotthard rail base tunnel, Switzerland. *Chemical Geology, 334*, 240–253.

Cinco, L.H., & Samaniego, F.V. (1977). Effect of wellbore storage and damage on the transient pressure behavior of vertically fractured wells. *Soc. Petrol. Engineers of AIME*, SPE 6752: 8, Dallas/Texas.

Clauser, C. (1992). Permeability of crystalline rocks. *EOS Transactions of the American Geophysical Union, 73*, 233–237.

Cooper, H. H., & Jacob, C. E. (1946). A generalized graphical method for evaluating formation constants and summarizing well field history. *American Geophysical Union Transaction., 27*, 526–534.

Correns, C.W. (1956). The geochemistry of the halogens. In Ahrens et al. (eds.), *Physics and Chemistry of the Earth*, vol. 1, (pp. 181–233), New York: McGraw-Hill.

Dezayes, C., & Lerouge, C. (2019). Reconstructing paleofluid circulation at the hercynian basement/mesozoic sedimentary cover interface in the upper rhine graben. *Geofluids*. 1-30. https://doi.org/10.1155/2019/4849860.

Dèzes, P., Schmid, S. M., & Ziegler, P. A. (2004). Evolution to the European Cenozoic Rift System: Interaction of the Alpine and Pyrenean orogens with their foreland lithosphere. *Tectonophysics, 389*, 1–33.

Drüppel, K., Stober, I., Grimmer, J.C., & Mertz-Kraus, R. (2020). Experimental alteration of granitic rocks: Implications for the evolution of geothermal brines in the Upper Rhine Graben, Germany. *Geothermics*, 88. https://doi.org/10.1016/j.geothermics.2020.101903.

Edmunds, W. M., & Savage, D. (1991). Geochemical characteristics of groundwater in granites and related crystalline rocks. In R. A. Downing & W. B. Wilkinson (Eds.), *Applied Groundwater Hydrology, a British Perspective* (pp. 199–216). Clarendon Press.

Emmermann, R., Althaus, E., Giese, P., & Stöckert, B. (1995). KTB Hauptbohrung: Results of Geosientific Investigation in the KTB Field Laboratory, Final Report: 0–9,101 m. *KTB Report*, 95-2, E. Stuttgart: Schweizerbart'sche Verlagsbuchhandlung.

Frape, S.K., & Fritz, P. (1987). Geochemical trends for groundwaters from the Canadian Shield. In Fritz, P., Frape, S.K (eds.), *Saline Water and Gases in Crystalline Rocks, Geological Association of Canada Special Paper, 33* (pp. 19–38). Ottawa: The Runge Press Ltd.

Frape, S.K., Blyth, A., Blomqvist, R., McNutt, R.H., & Gascoyne, M. (2004). Deep fluids in the continents: II. Crystalline rocks. In Drever, J.I., Holland, H.D., & Turekian, K.K. (eds.), *Surface and Ground Water, Weathering, and Soils, Treatise on Geochemistry* (pp. 541–580). Amsterdam: Elsevier.

Genter, A., Evans, K., Cuenot, N., Fritsch, D., & Sanjuan, B. (2010). Contribution of the exploration of deep crystalline fractured reservoir of Soultz to the knowledge of enhanced geothermal systems (EGS). *Comptes Rendus Geosience, 342*(7–8), 502–516. https://doi.org/10.1016/j.crte.2010.01.006

Geothermal Explorers Ltd. (2006). Cleanout and stimulation programme Basel 1 (BS1). report of Geothermal Explorers Ltd., 98. https://www.wsu.bs.ch. Accessed 24 May 2021.

Grimaud, D., Beaucaire, C., & Michard, G. (1990). Modelling of the evolution of ground waters in a granite system at low temperature: The Stripa ground waters, Sweden. *Applied Geochemistry, 5*, 515–525.

Häring, M.O., Ladner, F., Schanz, U., & Spillmann, T. (2008a) Deep-Heat-Mining Basel, Preliminary results. *Report Geothermal Explorers Ltd*, 9 p., Pratteln Switzerland.

Häring, M. O., Schanz, U., Ladner, F., & Dyer, B. C. (2008). Characterisation of the Basel 1 enhanced geothermal system. *Geothermics, 37*, 469–495.

Hofer, M. (2015). Gesteine und Tiefenwässer des Deep-Heat-Mining Projektes in Basel. Bachelor thesis, 52 p., University of Freiburg.
Holl, H.-G. (2015). What did we learn about EGS in the Cooper Basin?. *Report Geodynamic ltd*, Report no.: RES-FN-OT-RPT-01179, p. 78, https://doi.org/10.13140/RG.2.2.33547.49443.
Holland, T. J. B., & Powell, R. (2011). An improved and extended internally consistent thermodynamic dataset for phases of petrological interest, involving a new equation of state for solids. *Journal of Metamorphic Geology, 29*, 333–383.
Horner, D.R. (1951). Pressure Built-up in Wells. 3rd World Petroleum Congress, Sect. II, *E. J. Bull.*, WPC-413, 503–521, The Hague, The Netherlands.
Ingebritsen, S. E., & Manning, C. E. (1999). Geological implications of a permeability-depth curve for the continental crust. *Geology, 27*, 1107–1110.
Kaeser, B., Kalt, A., & Borel, J. (2007). The crystalline basement drilled at the Basel-1 geothermal site. A preliminary petrological geochemical study. Institut de Géologie et d'Hydrogéologie, Université de Neuchâtel. Internal report, 45 pp, Neuchâtel, Switzerland.
Kozlovsky, Y. E. A. (1987). *The Superdeep Well of the Kola Peninsula*. New York: Springer Press.
Ladner, F., & Häring, M. O. (2009). Hydraulic characteristics of the basel 1 enhanced geothermal system. *GRC Transactions, 33*, 199–203.
Ladner, F., Schanz, U., & Häring, M. O. (2008). Deep-Heat-Mining-Projekt Basel—Erste Erkenntnisse bei der Entwicklung eines Enhanced Geothermal System (EGS). *Bulletin Angew Geology, 13*(1), 41–54.
Laubscher, H. (2001). Plate interactions at the southern end of the Rhine graben. *Tectonophysics, 343*, 1–19.
Manning, C. E., & Ingebritsen, S. E. (1999). Permeability of the continental crust: Implications of geothermal data and metamorphic systems. *Reviews of Geophysics, 37*, 127–150.
Markl, G., & Bucher, K. (1998). Metamorphic salt in granulites: Implications for the presence and composition of fluids in the lower crust. *Nature, 391*, 781–783.
Mullis, J. (1987). Fluideinschluss-Untersuchungen in den Nagra-Bohrungen der Nordschweiz. *Ecology Geology Helv., 80*, 553–568.
Orville, P. M. (1972). Plagioclase cation exchange equilibria with aqueous chloride solution: Results at 700 °C and 2000 bars in the presence of quartz. *American Journal of Science, 272*, 234–272.
Parkhurst, D.L., & Appelo, C.A.J. (1999). User's guide to PHREEQC (Version 2)—a computer program for speciation, batch-reaction, one-dimensional transport and inverse geochemical calculations. *Water-Resources Investigations Report* 99-4259, U.S. Geological Survey, Denver, Colorado, p. 312.
Pauwels, H., Fouillac, C., & Fouillac, A.-M. (1993). Chemistry and isotopes of deep geothermal saline Fluids in the Upper Rhine Graben: Origin of compounds and water-rock interactions. *Geochimica Et Cosmochimica Acta, 57*, 2737–2749.
Pine, R. J., & Ledingham, P. (1983). In-situ hydraulic parameters for the Carnmenellis granite hot dry rock geothermal energy research reservoir. *SPE annual technical conference*, SPE12020, San Francisco, United States.
Pouchou, J. L., & Pichoir, F. (1991). Quantitative analysis of homogeneous or stratified microvolumes applying the model "PAP." In K. F. J. Heinrich & D. E. Newbury (Eds.), *Electron Probe Quantitation* (pp. 31–75). Springer.
Sanjuan, B., Millot, R., Innocent, C., Dezayes, C., Scheiber, J., & Brach, M. (2016). Major geochemical characteristics of geothermal brines from the Upper Rhine Graben granitic basement with constraints on temperature and circulation. *Chemical Geology, 428*, 27–47.
Solberg, P., Lockner, D., & Byerlee, J.D. (1980). Hydraulic Fracturing in Granite under Geothermal Conditions. *International Journal of Rock Mechanics and Mining Science and Geomechanics*, 17, 25–33, Pergamon Press Ltd, UK.
Stober, I. (1986). Strömungsverhalten in Festgesteinsaquiferen mit Hilfe von Pump- und Injektionsversuchen. *Geologisches Jahrbuch*, C 42, 204 S., Hannover.
Stober, I., Giovanoli, F., Wiebe, V. & Bucher, K. (2022). Deep hydrochemical section through the Central Alps—evolution of deep water in the continental upper crust and solute acquisition during water-rock-interaction along the Sedrun section of the Gotthard Base Tunnel. *Swiss Journal of Geosciences* (under review).
Stober, I. (2011). Depth- and pressure-dependent permeability in the upper continental crust: Data from the Urach 3 geothermal borehole, southwest Germany. *Hydrogeology Journal, 19*, 685–699.
Stober, I., & Bucher, K. (1999a). Deep Groundwater in the crystalline basement of the Black Forest region. *Applied Geochemistry, 14*, 237–254.
Stober, I., & Bucher, K. (1999b). Origin of salinity of deep groundwater in Crystalline rocks. *Terra Nova, 11*(4), 181–185.
Stober, I., & Bucher, K. (2000). Hydraulic properties of the upper continental crust: Data from the Urach 3 geothermal well. In I. Stober & K. Bucher (Eds.), *Hydrogeology in crystalline rocks* (pp. 53–78). KLUWER academic Publishers.
Stober, I., & Bucher, K. (2004). Fluid Sinks within the Earth's Crust. *Geofluids, 4*, 143–151.
Stober, I., & Bucher, K. (2005). The upper continental crust, an aquifer and its fluid: Hydraulic and chemical data from 4 km depth in fractured crystalline basement rocks at the KTB test site. *Geofluids, 5*, 8–19.
Stober, I., & Bucher, K. (2006). Hydraulic properties of the crystalline basement. *Hydrogeology Journal, 15*, 213–224.
Stober, I., & Bucher, K. (2014). Hydraulic conductivity of fractured upper crust: Insights from hydraulic tests in boreholes and fluid–rock interaction in crystalline basement rocks. *Geofluids, 16*, 161–178.
Stober, I., & Bucher, K. (2021). *Geothermal energy* (2nd ed.). Springer.
Stumm, W., & Morgan, J. J. (1975). *Aquatic Chemistry* (2nd ed.). Wiley and Sons.
Tischner, T., Pfender, M., & Teza, D. (2006). Hot Dry Rock Projekt Soultz: Erste Phase der Erstellung einer wissenschaftlichen Pilotanlage. *Abschlussbericht zum Vorhaben 0327097*, 87, BGR, Hannover.
Ustazewski, K., & Schmid, S. M. (2007). Latest Pliocene to recent thick-skinned tectonics at the Upper Rhine Graben-Jura Mountains junction. *Swiss Journal of Geosciences, 100*(2), 293–312.
Vidal, J., & Genter, A. (2018). Overview of naturally permeable fractured reservoirs in the central and southern Upper Rhine Graben: Insights from geothermal wells. *Geothermics, 74*, 57–73.
Weisenberger, T., & Bucher, K. (2010). Zeolites in fissures of granites and gneisses of the Central Alps. *Journal of Metamorphic Geology, 28*, 825–847.
Whitney, D. L., & Evans, B. W. (2010). Abbreviations for names of rock-forming minerals. *American Mineralogist, 95*, 185–187.
Wolery, T.J. (1992). EQ3/6, a Software Package for Geochemical Modelling of Aqueous Systems: Package Overview and Installation Guide. *Lawrence Livermore National Laboratory*, Livermore, California.
Yardley, B. W. D., & Banks, D. A. (1995). The behavior of chloride and bromide during metamorphic cycle. In Y. K. Kharaka & A. S. Maest (Eds.), *Water–Rock Interaction* (pp. 625–628). Balkema.
Zeitlhöfler, M., Wagner, B., & Spörlein, T. (2015). Strukturgeologie und Grundwasserführung im ostbayerischen Grundgebirge. *Geologica Bavarica, 112*, 1–64.
Ziegler, M., Valley, B., & Evans, K.F. (2015). Characterisation of Natural Fractures and Fracture Zones of the Basel EGS Reservoir inferred from Geophysical Logging of the Basel-1 Well. *Proceedings World Geothermal Congress*, 12 p., Melbourne, Australia.
Zimmer, K., Zhang, Y., Lu, P., Chen, Y., Zhang, G., Dalkilic, M., & Zhu, Ch. (2016). SUPCRTBL: A revised and extended thermodynamic dataset and software package of SUPCRT92. *Computers and Geosciences, 90*, 97–111.

## Publisher's Note